JOURNAL OF AIRCRAFT
Vol. 35, No. 2, March–April 1998

Active Control of Aircraft Cabin Noise Using Collocated Structural Actuators and Sensors

A. Grewal,* F. Nitzsche,* and D. G. Zimcik†
National Research Council, Ottawa, Ontario K1A 0R6, Canada
and
B. Leigh‡
De Havilland, Inc., Downsview, Ontario M3K 1Y5, Canada

This paper describes preliminary laboratory experiments conducted on a turboprop aircraft fuselage to reduce propeller-induced tonal cabin noise and vibration. Piezoelectric elements were grouped to construct a long one-dimensional array of actuators bonded to the fuselage in the main sound transmission path at the propeller footprint. Strain gauges and accelerometers were used as alternative sensor devices and were distributed along the actuator in a collocated arrangement. The array of actuators and sensors was designed to work in unison, generating a smart closed-loop array of control elements that possess wave-number filtering properties for the less critical acoustic modes of the cabin. The control system was tested in the laboratory using a simplified propeller pressure loading distribution. Promising results were obtained, as the closed-loop control system proved to be unconditionally stable and capable of significantly attenuating the fuselage vibration in the transmission path at the critical blade passage frequencies. Moreover, although only one array of control elements was used, interior noise reduction was also observed during the tests, proving the merit of the concept.

Nomenclature

s = Laplace variable
α = compensator gain
ζ_c = compensator damping ratio
ϕ_c = compensator phase
ω_c = control frequency

Introduction

THERE is a desire to reduce cabin noise in commercial turboprop aircraft using techniques of active noise control. The sources of noise in a turboprop aircraft include boundary-layer noise, structure-borne noise from engine vibration, and acoustic excitation of the fuselage caused by the propeller, with the latter being dominant for most turboprop aircraft.[1] The excitation is predominantly narrow band in nature, concentrated at multiples of the blade passage frequency (BPF) of the propeller. There is considerable interest in developing reliable, low-cost, and lightweight solutions to reduce the interior cabin noise and vibration levels, with improved passenger comfort being the primary motivation.

Possible noise reduction approaches encompass passive methods, such as structural modification,[2] damping treatment,[3–5] and active methods, which range from synchrophasing to control of either the acoustic field[6–8] or the structural (vibration) transmission path.[9,10] However, there are a number of problems associated with passive methods of noise reduction. For example, stiffening the fuselage may result in a large weight penalty, while broadband passive damping is ineffective because the propeller excitation is generally forced rather than resonant. The use of tuned vibration absorbers (TVA) has yielded significant reductions at selected frequencies,[3] but there is a problem in keeping the TVAs tuned in a changing environment. Using an active approach, however, the control system can be designed to cope with changing operating conditions. Currently, various turboprop aircraft manufacturers offer active noise control systems as standard or optional equipment on their aircraft. There are some limitations with these systems, such as their reliance on a large number of microphones and speakers, the localized nature of noise reduction, and reports of increased levels of floor vibration, which degrades the overall passenger comfort level. These factors have contributed to the continued interest in seeking alternative solutions to noise reduction in turboprop aircraft.

An alternative approach to active noise control of turboprop aircraft discussed in this paper is to weaken the coupling between the exterior and interior acoustics. In this approach, the transmission of sound is impaired before it enters the cabin. This is consistent with the well-accepted rule that treating noise at or close to its source yields performance superior to treating the problem farther down the transmission path. The resulting system is generally simpler, with fewer actuators and sensors, as they are required only in the propeller footprint area.[11,12] The concept of achieving noise reduction through the active control of structural vibrations is not new. However, most of these concepts rely on the feedback of interior acoustical information. In contrast, the approach followed in this investigation involves the feedback of local structural vibration to achieve a reduction of sound transmission, through the use of piezoelectric actuators mounted on the fuselage to control the propeller-induced vibrations. Results of noise and vibration control experiments on a full-scale de Havilland Dash-8 fuselage are presented.

Control Strategy

The approach taken in this work is one of reducing the transmission of noise by controlling structural vibration. Piezoelectric actuators, which are bonded to the fuselage, provide the

Presented as Paper 96-1274 at the AIAA/ASME/AHS Adaptive Structures Forum, Salt Lake City, UT, April 18–19, 1996; received Aug. 5, 1996; revision received Oct. 7, 1997; accepted for publication Oct. 10, 1997.

*Research Officer, Institute for Aerospace Research, Montreal Road. Member AIAA.
†Group Leader, Institute for Aerospace Research, Montreal Road. Member AIAA.
‡Group Leader, Structures Research and Development. Member AIAA.

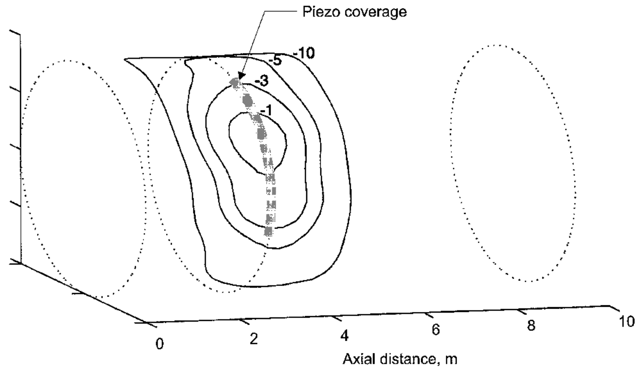

Fig. 1 Port-side propeller pressure in decibels in relation to maximum value. The propeller plane and the force and aft bulkheads are also indicated.

necessary control inputs, while strain gauges and accelerometers are used as sensors. The use of structure-mounted actuators and sensors offers distinct advantages over the use of speakers and microphones in the passenger cabin. For example, the actuators and sensors can be placed directly on the airframe, without having to make room in the passenger cabin for speakers and microphones. Moreover, because the acoustic disturbance from the propellers is concentrated in a relatively compact area of the aircraft fuselage, actuators only have to be placed in the neighborhood of this area. The external sound pressure distribution for the Dash-8 aircraft at the BPF is shown in Fig. 1.

In addition to these practical advantages, the use of structural sensors and actuators has other advantages. The task of obtaining transfer functions between secondary acoustic sources, i.e., control speakers, and microphones is obviated. This is a considerable factor, as transfer functions involving internal sound pressure may vary considerably with changes in passenger load and operating conditions, whereas the fundamental characteristics of the local structural transfer functions remain unchanged. Thus, the resulting control laws will be more robust. This is particularly true if collocated strain sensors are used because the resulting transfer functions will be positive–real, and positive–real feedback can be used, ensuring stability.[13]

Employing structural control to achieve a reduction in transmitted noise is not without disadvantages and challenges. These include the relatively high voltages required for control, the simultaneous need for thin bond lines to minimize shear losses and strong adhesion to the fuselage, and the requirement to identify and subsequently sense and control only those modes of vibration that couple well with the cabin acoustical field.

The interior acoustic response does not couple well with high wave number structural vibrations at frequencies of interest.[14] Therefore, a number of small piezoelectric elements are connected electrically to act as one larger actuator, with overall length comparable to one-half the acoustic wavelength of interest. Thus, the actuator acts as a wave number filter[15] that filters out the high wave number vibrations that do not couple to the acoustic field. A similar sensor arrangement will provide additional wave number filtering. This addresses a problem observed with other structural control approaches to active noise control, where a reduction in acoustic transmission was not observed when the direct control objective was minimizing structural energy.[16] Although compact, the distributed nature of the propeller noise field still requires a number of distinct actuators to achieve control authority. This leads to several options for the overall control architecture. A purely decentralized control scheme, where each actuator employs only single input/single output (SISO) feedback of collocated information, has numerous advantages. The resulting system is modular, with low computing requirements and associated weight penalty. Control system redesign is minimized when additional sensor–actuator pairs are required, and graceful performance degradation results from single-point failures. Each SISO control loop can be tuned using readily available tachometer information from the turboprops.

Because the BPF and a few higher harmonics dominate the interior noise spectrum, noise control at these discrete frequencies is desired. Narrow-band control for each of these frequencies can be accomplished independently. At the lower harmonics, the propeller pressure distribution extends over a larger area, making the problem more difficult and necessitating the use of significantly more piezoelectric material. However, at these frequencies, the coupling between structural vibration and interior acoustics is also less complex. For the present study, with its principal objective being preliminary verification of the noise control approach, the higher harmonics of the BPF, i.e., 210 and 280 Hz, were targeted.

Actuators and Sensors

Because of their large force generating, high bandwidth, and relatively low mass properties, piezoelectric materials are well suited for vibration control applications. Moreover, the spatially distributed nature of the resulting applied forces reduces the effect on high wave number modes, which are not efficient radiators of sound. Thus, the energy employed in control is expended efficiently, insofar as sound transmission attenuation is concerned.

The spatial distribution of the propeller noise field impinging on the fuselage contributes significantly to its structural response. For example, for a force distribution that has uniform phase and magnitude over a particular region, the modes that are excited are typically ones that possess half-waves in the axial and circumferential directions that approximately match (geometrically) the pressure distribution. Of course, for pressure distributions with spatially varying phase and magnitude, this relationship is much more complex. Nevertheless, the spatial extent of the pressure plays a major role in determining the dominant modes that are excited. In an analogous fashion, the spatial extent of the piezoelectric elements also determines which modes can be controlled by the actuator. Therefore, the coverage of the piezoelectric actuator elements should encompass the region of high propeller pressure.

A judicious choice of sensors can simplify the control design procedure, which requires a transfer function model between actuator and sensor. By sensing fuselage strains that are ap proximately collocated with the actuators, the transfer function between them becomes relatively simple because of the duality of the sensor–actuator pair. Another important aspect of the sensor is that its output must be well correlated to the performance variable (interior sound levels). The minimization of the sensed variable must ensure that noise transmission is also being minimized. In a manner analogous to the size of the actuator, the sensor must also be spatially distributed to be insensitive to high wave number vibrations, while being responsive to the acoustically critical low wave number vibrations. This is ideally accomplished by the use of distributed sensors constructed from polyvinylidene fluoride (PVDF) film, for example. For these experiments, however, discrete structural sensors (strain gauges and accelerometers) distributed over the length of the actuator were used. In a true distributed sensor, a weighted average of the sensed quantity over the spatial extent of the sensor is produced at the physical level. The weighting can be provided by shaping the width or thickness of the sensor. Conversely, the electrical signals from each discrete sensor can be averaged in a weighted sense by the controller to provide a single equivalent sensed variable. It can be shown that the weighting terms of the discrete sensors can be selected to approximate the response of a given distributed sensor. Note that both an array of discrete sensors and a distributed sensor may be insensitive to certain modes of vibration. For example, a distributed sensor symmetric in its sensitivity about its centerline will be relatively unresponsive to a mode that is antisymmetric about the sensor centerline as a result of the canceling of signal contributions from either half of the sensor. Similarly, an array of discrete sensors distributed and weighted symmetrically over the same region will also be unresponsive to antisymmetric vibration modes.

Because the aircraft engine speed varies during flight, it should be available to the controller through the tachometer signal in actual implementation. For the present work, the disturbance frequency was assumed to be constant. If the frequency of the disturbance were directly available, then the control law could be easily modified to use this information through continuous gain scheduling.

Control Design

Most of the current research in active noise control uses some variation of the least mean square adaptive disturbance feedforward algorithm.[17] This algorithm requires both the disturbance signal and the error signal. Classical or modern control theory can also be used to develop feedback control systems. Although the details in implementation of feedback and feedforward systems differ, both approaches can be viewed as being equivalent in that they introduce high gain feedback of the sensor output at the disturbance frequency.[18–20] This results in a low value of the sensitivity transfer function, i.e., disturbance to sensor output, at the prescribed frequency.

An analog I/O board was used in conjunction with an 80486 host personal computer for real-time control. A sampling rate of approximately 3 kHz, or 10 times faster than the frequency of the highest controlled harmonic, was employed. In actual implementation, the control algorithm may be implemented in analog circuits to reduce the size and weight requirements. Alternatively, the use of a digital signal processor board will allow for the implementation of relatively complex controller models.

Experimental Setup

The experimental aircraft was a de Havilland Dash-8 Series 100 fuselage without wings and empennage (Fig. 2). The interior was green, that is, there were no seats or trim, although the internal insulation was present. As a result, there was less acoustic and structural damping than would be present in an actual aircraft. The aircraft was supported during the tests by an overhead crane attached to the fore and aft edges of the wing box on either side of the fuselage. The aircraft was prevented from swinging by either a foam-lined cradle or by the foam-lined support stands visible in Fig. 2. This support system provides a reproducible method of supporting the aircraft that is to some degree representative of steady-state loading present during flight, i.e., the fuselage is supported by the wing box both in flight and in the experiments. A schematic diagram of the experimental setup is shown in Fig. 3.

A piezoelectric actuator is capable of inducing more strain into the host structure if its extensional stiffness is large. The problem of controlling aircraft fuselage vibration caused by propeller noise is challenging, because of both the vibration levels present and the relatively high stiffness of the fuselage in comparison to other piezoelectric control applications, such

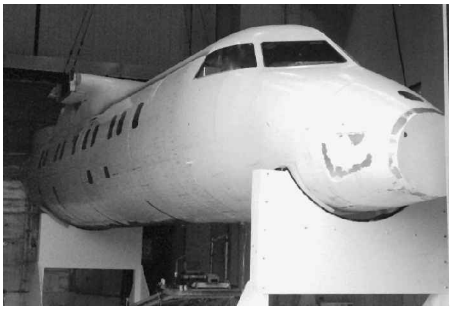

Fig. 2 De Havilland Dash-8 aircraft fuselage used for testing.

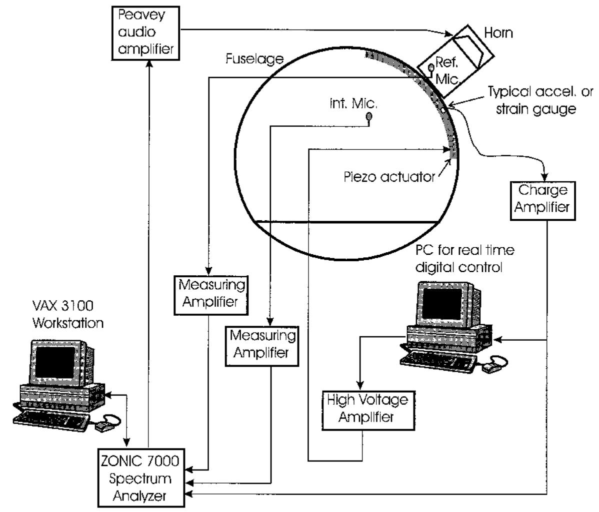

Fig. 3 Schematic of experimental setup and control system.

as flexible space structures. The properties of the piezoelectric actuator material used (Ai-8) are: 1) piezoelectric strain constant $d_{31} = 1.05 \times 10^{-10}$ C/N, 2) modulus of elasticity $E = 82 \times 10^{9}$ Pa, and 3) cross-sectional area $A = 0.805$ cm^2. This particular piezoelectric, which had a high stiffness and a thick cross section, was therefore suited for this particular problem. However, because the total added mass is important, actuator dimensions should be chosen no larger than needed. This implies that the piezoelectric actuators should be stiffness-matched with the structure to which they are bonded, to get the most effective actuator for minimum mass. The individual actuator element was chosen to minimize the bond line thickness, and therefore the loss of actuator effectiveness, resulting from the attachment of the flat piezoelectric elements to the curved fuselage. In actual implementation, it may prove feasible to machine the actuators to provide a curved surface that would allow an increase in the element length.

For the present study, piezoelectric elements were electrically connected in parallel to form a one-dimensional actuator approximately 1.6 m long, covering approximately a 70-deg arc on the fuselage. Structural sensors were attached between individual actuator elements. Continuous coverage was not always possible because of the presence of structural features on the fuselage. Preliminary vibroacoustic modeling of the problem using available flight pressure data indicated that the actuator was capable of canceling the resulting vibration levels with moderately high applied voltages (approximately 350 V).[21] In actual implementation, the required voltages can be reduced by using stacked or layered piezoelectric actuators. Overall power requirements were actually quite small because the piezoelectric impedance is primarily capacitive. A Trek HV Model 50/750 amplifier capable of producing 1500 V in unipolar operation was used. The actuators were bonded to the fuselage using a conductive epoxy (Bipax BA-2902). This allowed the fuselage itself to be used as a common ground plane for all actuators, and avoided the difficulty of making an electrical connection to the lower actuator surface without interfering with the bond.

Piezoelectric strain gauges (SG) were also employed as one of the two types of structural sensors. For these experiments, a total of three SGs were used, one placed approximately at the middle of the upper third of the actuators, one at the center of the actuators, and one at the bottom of the actuator array. The SGs were mounted with a nonconductive epoxy, as attaching wires to the lower electrical surface was simplified by the design of the gauge.

Accelerometers were used as the second type of sensor. These were attached at various locations, mainly in the actuator plane on the fuselage. Because the internal noise is transmitted principally by flexural (radial) vibration, the accelerometer measured a quantity in some sense closer to the desired performance metric (internal noise) than the SGs. However, the transfer function between actuator and sensor became more complicated, although measurements taken in this experiment indicated that this might not be a significant problem.

The noise attenuation performance of the control system was monitored by a microphone, placed at the head height of a seated passenger in the window row in the propeller plane on the port side. This is generally the seat location at which the greatest reductions are desired.

Because the objective at this stage was to demonstrate that the approach reduced the noise measured inside the aircraft, piezoelectric actuators did not cover the entire propeller footprint area of the aircraft in this feasibility study. Rather, a localized controlled excitation system was used, as shown schematically in Fig. 3. This horn directed sound from a loudspeaker to an area on the fuselage surface measuring 21.5 × 5 in. As a result of the small area of acoustic excitation, higher wave number modes are likely to be excited when compared to the case of actual flight-level propeller excitation. In future work, a multispeaker sound source will be used for improved simulation of the propeller field. The sensor output was fed back through the real-time control computer and the high-voltage amplifier to the piezoelectric actuator.

The SISO classical feedback algorithm implemented is of the form

$$K(s) = \alpha \frac{a + bs}{s^2 + 2\zeta_c\omega_c s + \omega_c^2} \tag{1}$$

The design parameters are α, the desired ω_c, ζ_c, and ϕ_c at the control frequency, which is related to a, b, and ω_c by the following equations:

$$a = \cos^{-1}\phi_c \tag{2}$$

$$b = \sin^{-1}\phi_c/\omega_c \tag{3}$$

The damping factor ζ_c effectively sets the bandwidth, and the overall gain together with the damping factor determine the peak gain. The overall system stability is determined by ϕ_c. In practice, values for each parameter are selected by examining the resulting loop transfer function. The controller is implemented in real time by representing and programming the compensator equations in discrete-time state–space form.

Experimental Results

The important open-loop transfer functions between the actuator and the output variables (strain and acceleration), and between the actuator and the true performance variable (interior sound), were measured.

The transfer functions were obtained by generating a band-limited white noise signal (27–624 Hz) of amplitude 2 V (peak) and passing it through the Trek amplifier (gain = 200 V/V) before applying it to the actuator array of piezoelectric elements. The sensor measurements were appropriately conditioned, either by charge amplifiers for the case of accelerometer and SG signals, or by a measuring amplifier in the case of the microphone signals, which were used to monitor noise reduction performance. The transfer function between the piezoelectric actuator and the average strain is shown in Fig. 4. The results are represented in decibels in relation to 1 μ-strain/V, where V represents the voltage applied to the piezoelectric actuator.

The positive–real nature of the transfer function, based on the collocated and dual sensor–actuator pair, is clearly evident from the relatively passive nature of the Bode plot; the magnitude varies by less than 10 dB, and the maximum phase variation is less than 60 deg over the frequency range of 0–600 Hz. The interlaced transmission zeros and poles are also characteristic of systems with collocated and dual sensor–actuator pairs. Three modes, at approximately 63, 278, and 324 Hz, are clearly evident. The 63-Hz mode was identified in an experimental modal analysis study on the same fuselage.[22] This mode is basically a symmetric shell mode with a circumferential wave number of three, although it is distorted somewhat by the presence of the floor. The axial wave number could not be determined because of the relatively few axial planes measured.

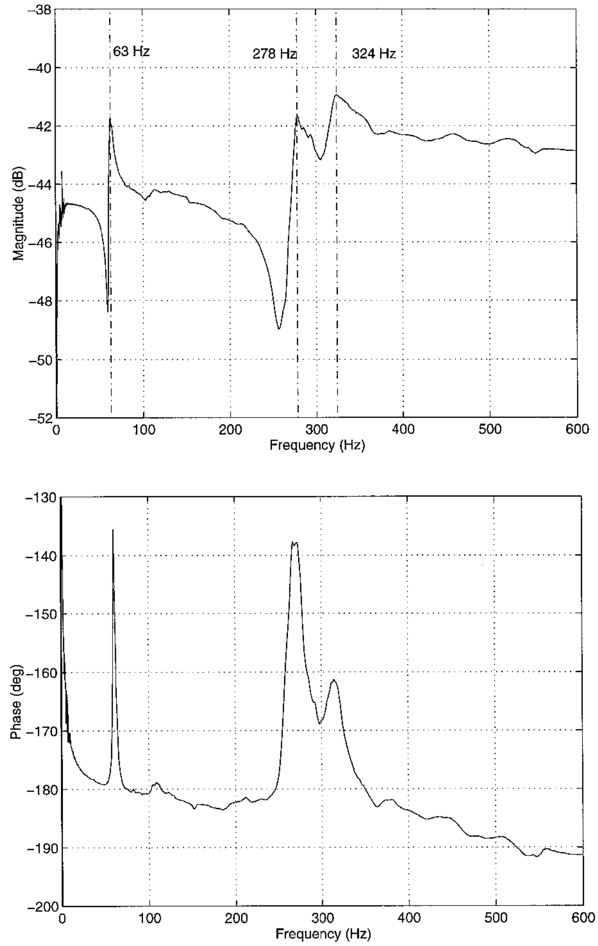

Fig. 4 Open-loop transfer function from piezoelectric actuator to average strain.

Open-loop transfer functions from the piezoelectric actuator to four accelerometers were also obtained. The four accelerometers were spaced approximately equally over the 1.6-m length of the actuator. The transfer function between the actuator and the average acceleration over the four locations is shown in Fig. 5 in decibels in relation to 1 ms^{-2}/V. Note the slight shifting of modal peaks when compared to the strain transfer function. As in the case of the average strain, the dynamics of the averaged signal are significantly less rich than the dynamics of the signals from the individual sensors. In this case, much of the resonant dynamics below approximately 250 Hz are not observable by the sensor. Because the actuator–sensor pair is now no longer dual, i.e., their product is not energy or power, the phase angle between them is not bounded by ±90 deg, as it was in the case of the piezoelectric actuator–SG combination. In fact, now the phase angle of the transfer function varies by more than 200 deg over the frequency range of 100–600 Hz. Moreover, the phase variations present in the individual accelerometer transfer functions (not shown) were much larger than for the averaged data, in some cases being greater than 900 deg over the previously stated frequency range. By contrast, the piezoelectric actuator-to-average strain

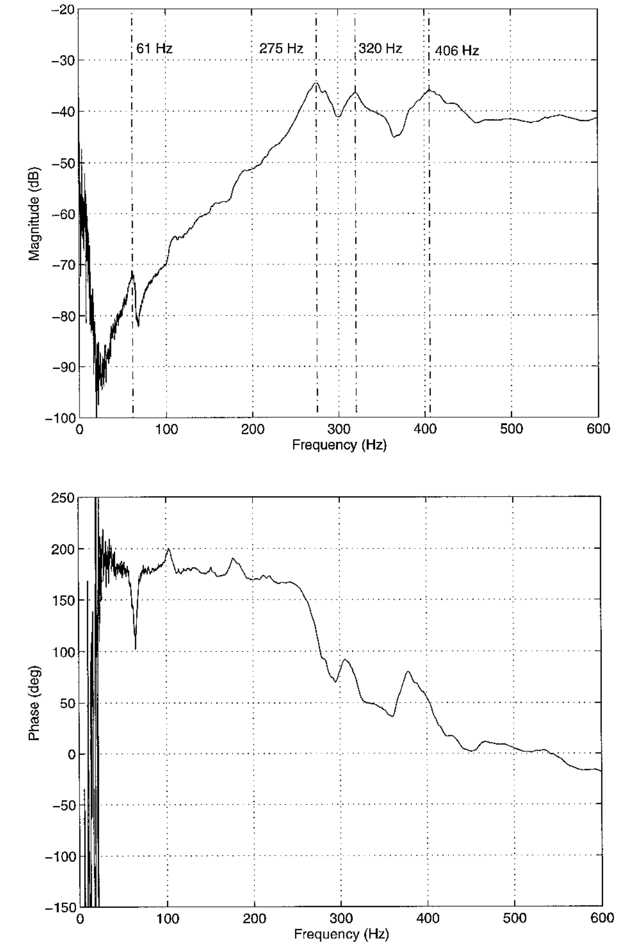

Fig. 5 Open-loop transfer function from piezoelectric actuator to average acceleration.

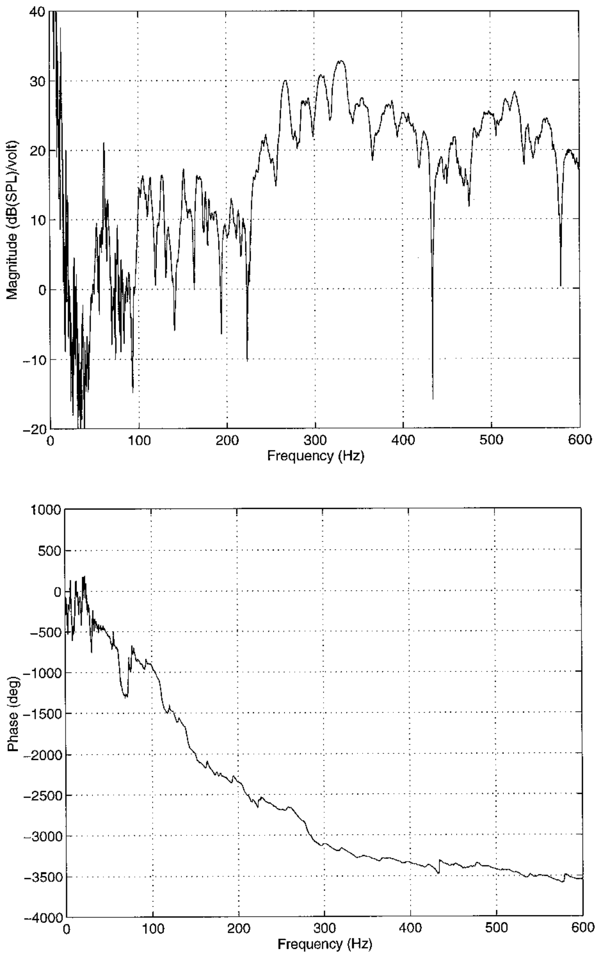

Fig. 6 Open-loop transfer function from piezoelectric actuator to the interior sound level.

transfer function had a phase variation of only 60 deg over the same frequency range.

The primary purpose of the preceding transfer function measurements is to quantify the extent to which the piezoelectric actuator is capable of inducing vibration in the fuselage at a location close to the acoustic disturbance, thus providing a measure of the effectiveness of the actuator. Another important measure of the effectiveness of the piezoelectric actuator is reflected in the transfer function from actuator to interior sound pressure level (SPL). For this measurement, a microphone was placed approximately at passenger ear height. The magnitude of the transfer function is expressed in decibels (SPL in relation to 20 μPa/V). From the results shown in Fig. 6, it can be seen that the maximum value of this transfer function occurs at about 330 Hz, where the magnitude is approximately 33 dB/V. For the present case, with an applied voltage of $\pm$400 V, this amounts to an SPL of approximately 85 dB, or 0.36 Pa (rms) at 330 Hz. This is a significant level of sound pressure compared with typical cabin sound pressure levels. It can be inferred that when the piezoelectric actuator is taken as a sound source, it is sufficiently strong to induce high sound pressure levels in the aircraft cabin and, therefore, through interference with the primary source, i.e., the disturbance, able to induce significant sound attenuation in the cabin.

Control at the fourth harmonic of the BPF (280 Hz) was investigated using both strain and acceleration feedback. The most promising results using strain feedback, from the point of view of both vibration suppression and noise transmission attenuation, were obtained with the feedback of two of the three SGs, the upper and the lower. This was probably because of the phase difference in response between the individual sensors. The measured loop transfer function for the system is shown in Fig. 7. The transfer function includes filters used both at the input to the I/O board for antialiasing, and at the output to reduce the spurious high-frequency noise of the D/A converter. The maximum gain achieved was 38 dB, and stability margins were approximately 4 dB in gain and 14 deg in phase.

A series of comparisons of open- and closed-loop performance in the presence of the acoustic disturbance was also made. First, the transfer functions from the exterior sound source (disturbance) to the measured variable (average of the upper and lower SGs) are presented (Fig. 8). The reduction in average strain at the control frequency (280 Hz) was about 38 dB, although a significant increase occurred at approximately 350 Hz.

All three SGs individually exhibited some reduction at the control frequency (280 Hz), as did the average of the three sensors. The closed- and open-loop sound transmissibility (exterior to interior SPLs), as expressed in decibels, is given in Fig. 9. The reduction at 280 Hz is 0.9 dB, whereas reductions of 9 and 13 dB are obtained at 286 and 290 Hz, respectively. These results are summarized in Table 1.

To evaluate the range of performance, control at a frequency of 210 Hz (3 $\times$ BPF) was also investigated. As was the case for 280 Hz, the most promising results were seen when the upper and lower strain gauges were averaged (with an equal weighting) to yield the sensed variable, although it must be added that an exhaustive search for the optimal combination of sensors and weighting factors was not undertaken. The compensator employed had a gain margin of approximately 10 dB, a phase margin of about 40 deg, and a maximum loop gain of 35 dB. A reduction in the average strain (upper and lower gauges) of 25 dB is obtained at 210 Hz (Fig. 10). The peak reduction, which is a few decibels higher, occurs at a fre-

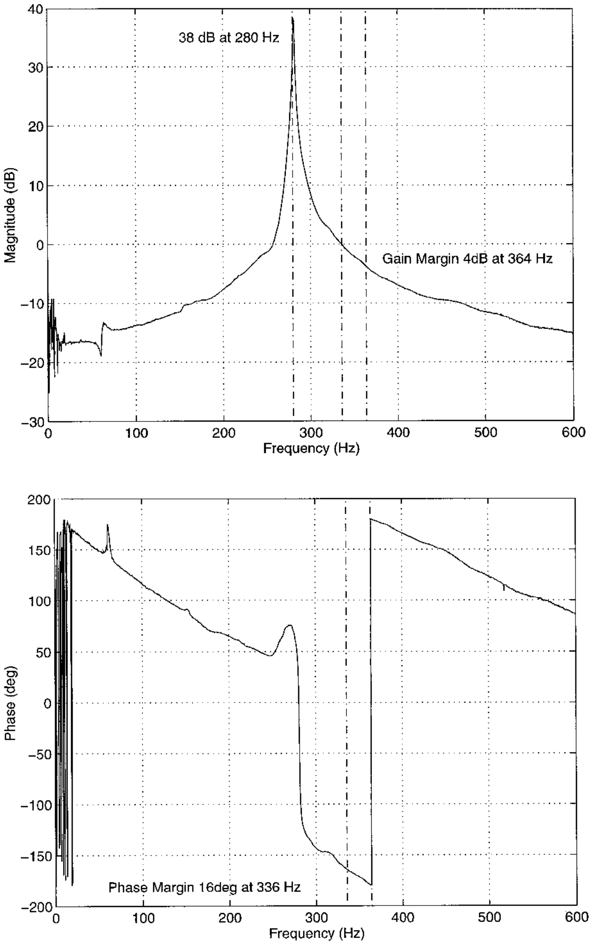

Fig. 7 Control-loop transfer function, control at 280 Hz, strain feedback.

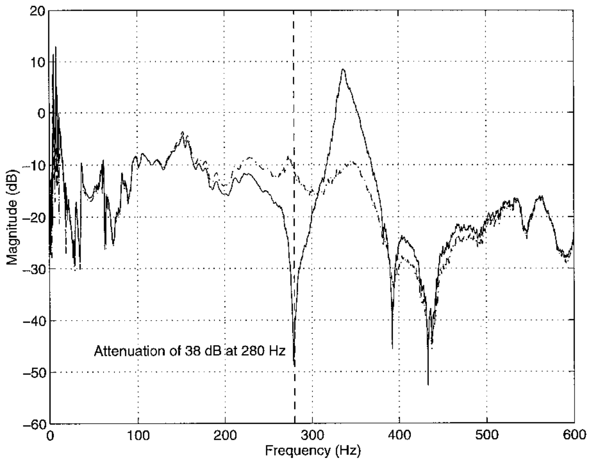

Fig. 8 Open- (dashed) and closed- (solid) loop transfer functions from exterior noise to average strain, strain feedback at 280 Hz.

Table 1 Summary of results obtained, strain feedback 280 Hz

Measured transfer functions (disturbance)	Frequency, Hz	Reduction, dB
Upper SG	280	0.8
Middle SG	280	10.8
Lower SG	280	13
Average strain (upper and lower SGs)	280	38
Average strain (all three SGs)	280	18
Interior sound	274	15
Interior sound	280	0.9
Interior sound	286	9
Interior sound	290	13

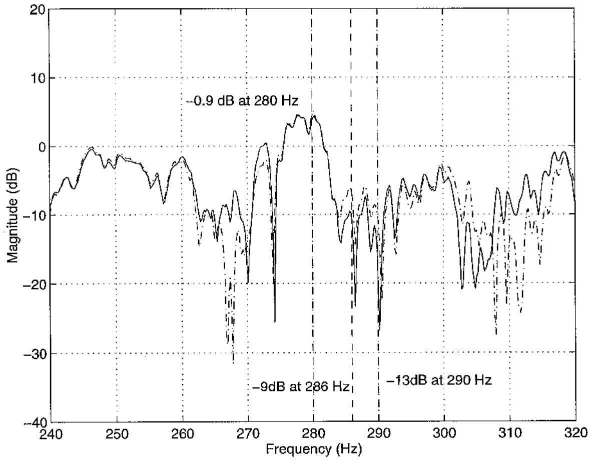

Fig. 9 Open- (dashed) and closed- (solid) loop transfer functions from exterior noise to interior sound pressure, strain feedback at 280 Hz.

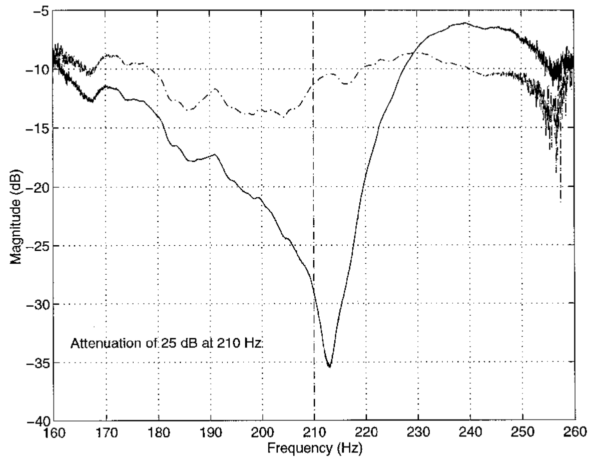

Fig. 10 Open- (dashed) and closed- (solid) loop transfer functions from exterior noise to average of upper and lower strain gauges, strain feedback at 210 Hz.

quency of approximately 213 Hz, whereas the sound attenuation at 210 Hz with the controller operating is only 0.5 dB (Fig. 11). The lack of strong correlation between attenuation in strain and interior noise reduction for control at 280 and 210 Hz could be a result of a number of factors. First, the coupling between the controlled vibration field and the acoustical field may be weak. Second, the localized nature of the control in vibration may be insufficient to reduce the vibration and hence sound transmission away from the actuated region of the fuselage. Last, the correlation between in-plane strain and interior noise is probably inherently weaker than between transverse (radial) vibration and interior noise. The last possibility is addressed next.

The use of acceleration feedback was investigated at a frequency of 280 Hz. As in the previous cases, various combinations of sensors and weighting factors were considered. In terms of sound attenuation, the most promising results were obtained when three accelerometers were used with their signals weighted equally. These accelerometers were attached to the fuselage at the same location as the three SGs described earlier. The resulting loop transfer function of the compensator–plant combination is shown in Fig. 12. As expected, the stability margins are lower than the cases when strain feedback

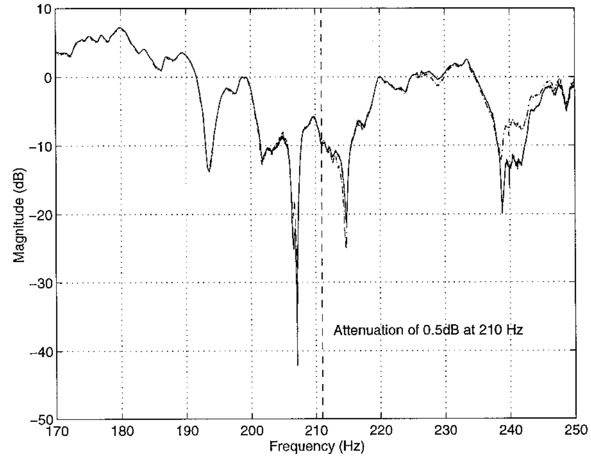

Fig. 11 Open- (dashed) and closed- (solid) loop transfer functions from exterior noise to interior sound pressure, strain feedback at 210 Hz.

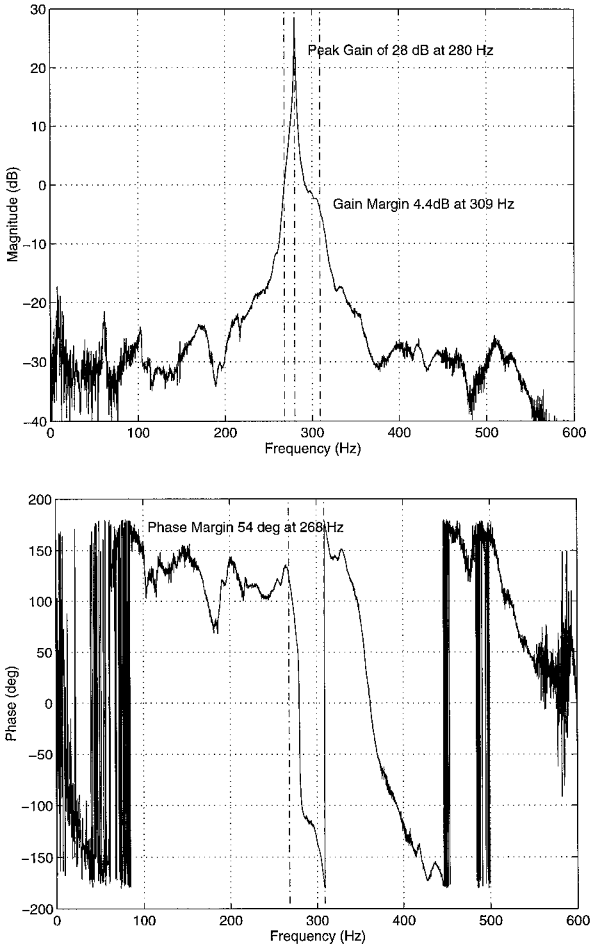

Fig. 12 Control-loop transfer function, control at 280 Hz, acceleration feedback.

was used because of the loss of the positive–real nature of the plant. The average acceleration does not exhibit a large reduction at the control frequency (Fig. 13); the reduction at 280 Hz is 0.2 dB. However, a larger reduction (10 dB) is seen at 275 Hz. A plot of the reductions in magnitude of the individual accelerometers provides more insight into the problem (Fig. 14). It can be seen that the upper accelerometer does experience a significant reduction (greater than 30 dB) at 280 Hz. However, the middle accelerometer exhibits a smaller reduction (approximately 4 dB), and the lower accelerometer actually exhibits a small increase in acceleration at that fre-

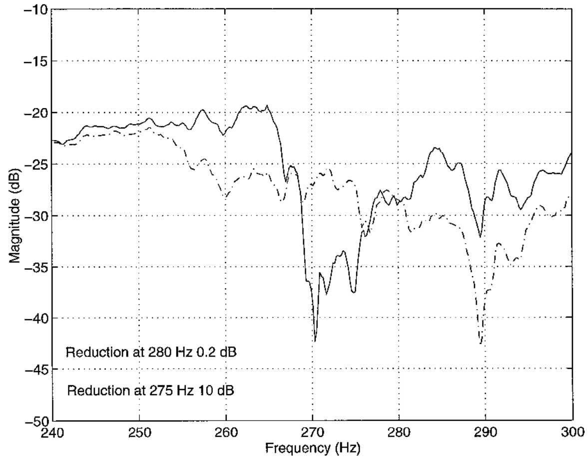

Fig. 13 Open- (dashed) and closed- (solid) loop transfer functions from exterior noise to average acceleration, acceleration feedback at 280 Hz.

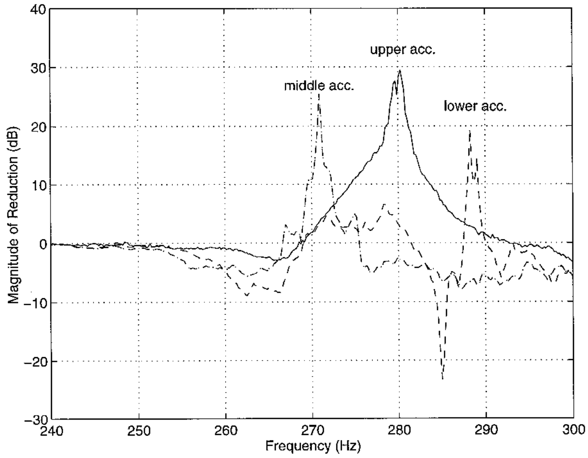

Fig. 14 Magnitude of individual accelerometer reductions with controller on, acceleration feedback at 280 Hz.

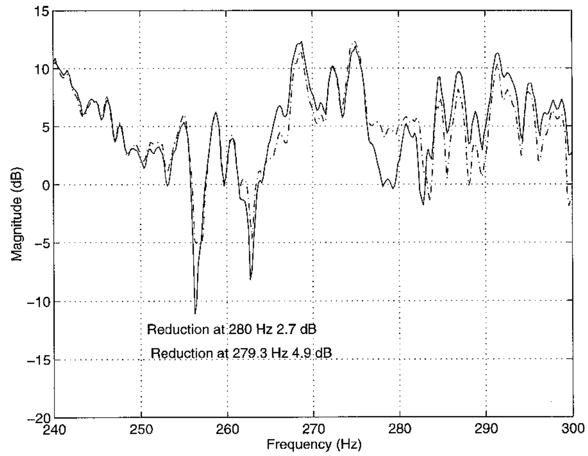

Fig. 15 Open- (dashed) and closed- (solid) loop transfer functions from exterior noise to interior sound pressure, acceleration feedback at 280 Hz.

quency. The level of open-loop vibration at the upper accelerometer is relatively low; therefore, its large reduction (closed-loop) does not contribute to a large reduction in the average acceleration.

The controller is successful in achieving sound attenuation, not only at the control frequency (2.7 dB), but also in the frequency range of 276–283 Hz (Fig. 15). There are two significant peak reductions in that range: at 279.3 Hz (4.9 dB) and at 282.4 Hz (5.7 dB). In reconciling the noise reduction with the vibration attenuation results, it can be inferred that the vibration in the region of the upper accelerometer and, to a lesser extent, the middle accelerometer contributes more to the interior noise than the vibration at the location of the lower accelerometer.

These results highlight the complicated nature of the coupling between the cabin acoustics and the fuselage structural response. The successful implementation of a noise control scheme employing structural feedback and control requires a good understanding of this relationship. Furthermore, the lack of reliable vibroacoustic models of aircraft requires the reliance on a primarily experimental approach to developing such active noise control systems. Both the dominant acoustic modes at the critical frequencies, and the structural modes that couple well with these dominant acoustic modes, must be determined. Effective control and sensing of these structural modes is probably the most critical aspect of implementing structurally based active noise control systems.

Conclusions

The feasibility of using piezoelectric actuators and collocated feedback in reducing the cabin noise environment and fuselage vibration levels in a Dash-8 turboprop aircraft has been shown. The reductions in fuselage vibration and cabin noise obtained in a limited implementation on an actual aircraft were significant. These reductions were achieved using a simple second-order classical compensator that is particularly suited for the use of strain feedback because of the positive–real nature of the actuator to SG transfer functions. However, the most promising results were obtained when acceleration feedback was employed. The peak sound attenuation achieved in this instance was 4.9 dB, and this result was obtained within a 1-Hz bandwidth of the target control frequency. The superior noise reduction performance achieved with acceleration feedback compared with strain feedback is consistent with the fact that the flexural (radial) vibration of the fuselage is the dominant mechanism for noise transmission. Because the in-plane strain consists of two components, extensional and flexural deformation, reductions in overall in-plane strain may be achieved by changes in the phase relationship between the constituent strains without a reduction in the flexural component. In such a scenario, the noise reduction would be insignificant.

References

[1]Mixson, J. S., and Powell, C. A., "Review of Recent Research on Interior Noise of Propeller Aircraft," AIAA Paper 84-2349, Oct. 1984.

[2]Bhat, R. B., Sobieszczanski, J., and Mixson, J. S., "Reduction of Aircraft Cabin Noise by Fuselage Structural Optimization," *Proceedings of the Technical Program, NOISEXPO: National Noise and Vibration Control Conference* (Chicago, IL), Acoustical Publications, Inc., Bay Village, OH, 1977, pp. 40–45.

[3]Waterman, E. H., Kaptein, D., and Sarin, S. L., "Fokker's Activities in Cabin Noise Control for Propeller Aircraft," Society of Automotive Engineers, Paper 830736, Warrendale, PA, April 1983.

[4]Halvorsen, W. G., and Emborg, U., "Interior Noise Control of the Saab 340 Aircraft," Society of Automotive Engineers, Paper 891080, Warrendale, PA, April 1989.

[5]Borchers, I. U., Hackstein, H. J., Bartles, P., Gruneweld, M., and Wenigwieser, C., "Summary of Dornier 328 Interior Noise Control Study," *Proceedings of the 1990 International Conference on Noise Control Engineering* (Gothenburg, Sweden), Acoustical Society of Sweden, Gothenburg, Sweden, 1990, pp. 811–816.

[6]Elliot, S. J., Nelson, P. A., Stothers, I. M., and Boucher, C. C., "In-Flight Experiments on the Active Control of Propeller-Induced Cabin Noise," *Journal of Sound and Vibration*, Vol. 140, No. 2, 1990, pp. 219–238.

[7]Warner, J. V., and Bernhard, R. J., "Digital Control of Local Sound Fields in an Aircraft Passenger Compartment," *AIAA Journal*, Vol. 28, No. 2, 1990, pp. 284–289.

[8]Borchers, I. U., Renger, K., Paillard, J., Billoud, G., Koers, P., and Doppenberg, E., "Selected Flight Test Data and Control System Results of the CEC BRITE/EURAM ASANCA Study," *Proceedings of the 1993 International Congress on Noise Control Engineering* (Leuven, Belgium), The Belgian Acoustical Association, Antwerp, Belgium, 1993, pp. 59–64.

[9]Simpson, M. A., Leong, T. M., Fuller, C. R., and Jones, J. D., "Full-Scale Demonstration Tests of Cabin Noise Reduction Using Active Vibration Control," *Journal of Aircraft*, Vol. 28, No. 3, 1991, pp. 208–215.

[10]Fuller, C. R., Snyder, S. D., Hansen, C. H., and Silcox, R. J., "Active Control of Interior Noise in Model Aircraft Fuselages Using Piezoceramic Actuators," *AIAA Journal*, Vol. 30, No. 11, 1992, pp. 2613–2617.

[11]Silcox, R. J., Fuller, C. R., and Lester, H. C., "Mechanisms of Active Control in Cylindrical Fuselage Structures," *AIAA Journal*, Vol. 28, No. 8, 1990, pp. 1397–1404.

[12]Rossetti, D. J., Norris, M. A., Southward, S. C., and Sun, J. Q., "A Comparison of Speakers and Structural-Based Actuators for Aircraft Cabin Noise Control," *2nd Conference on Recent Advances in Active Control of Sound and Vibration* (Blacksburg, VA), Technomic, Lancaster, PA, 1993, pp. S1–S10.

[13]Slater, G. L., Bosse, A. B., and Zhang, Q., "Robustness of Positive Real Controllers for Large Space Structures," *Journal of Guidance, Control, and Dynamics*, Vol. 15, No. 1, 1992, pp. 58–64.

[14]Fuller, C. R., and Burdisso, R. A., "A Wavenumber Domain Approach to the Active Control of Structure-Borne Sound," *Journal of Sound and Vibration*, Vol. 148, No. 2, 1991, pp. 355–360.

[15]Collins, S. A., Miller, D. W., and Von Flotow, A. H., "Distributed Sensors as Spatial Filters in Active Structural Control," *Journal of Sound and Vibration*, Vol. 173, No. 4, 1994, pp. 471–501.

[16]Thomas, D. R., Nelson, P. A., and Elliot, S. J., "Active Control of the Transmission of Sound Through a Thin Cylindrical Shell, Part I: The Minimization of Vibrational Energy," *Journal of Sound and Vibration*, Vol. 167, No. 1, 1993, pp. 91–111.

[17]Widrow, B., and Stearns, S. D., *Adaptive Signal Processing*, Prentice–Hall, Englewood Cliffs, NJ, 1985.

[18]Sievers, L. A., and Von Flotow, A. H., "Comparison and Extensions of Control Methods for Narrow-Band Disturbance Rejection," *IEEE Transactions on Signal Processing*, Vol. 40, No. 10, 1992, pp. 2377–2391.

[19]MacMartin, D. G., "A Feedback Perspective on the LMS Disturbance Feedforward Algorithm," *Proceedings of the 1994 American Control Conference* (Baltimore, MD), Inst. of Electrical and Electronics Engineers, New York, 1994, pp. 1632–1636.

[20]MacMartin, D., and Grewal, A., "Active Piezoelectric Vibration Control–Preliminary Analysis and Beam Experiments," National Research Council, TR LTR-ST-1987, Ottawa, ON, Canada, Feb. 1995.

[21]Grewal, A., and MacMartin, D., "Experiments on the Control of Aircraft Cabin Noise Using Piezoelectric Actuators," National Research Council, TR LTR-ST-2004, Ottawa, ON, Canada, April 1995.

[22]Grewal, A., and Hurtubise, L. C., "Experimental Modal Testing and Analysis of the de Havilland Dash-8 Series 100 Fuselage," National Research Council, TR LTR-ST-2067, Ottawa, ON, Canada, Dec. 1996.